

Crystal powder silver nanoparticles green synthesized, characterization, antibacterial and cytotoxicity effects

MANAL A. AWAD^{a,*}, AWATIF A. HENDI^b, KHALID M. O. ORTASHI^c, RABAB A. EL DIB^{d,e}

^aKing Abdullah Institute for Nanotechnology, King Saud University, KSA

^bPhysics Department, Faculty of Science, King Saud University, KSA

^cDepartment of Chemical Engineering, King Saud University, KSA

^dPharmacognosy Department, College of Pharmacy, King Saud University, KSA

^eDepartment of Pharmacognosy, College of Pharmacy, Helwan University, Helwan 11795, Egypt

We described a simple, cost effective, non-toxic and environmental friendly green- chemistry reduction method to synthesized crystal nano silver (AgNPs) powder using CTAB and orange peel extract as reducing agent. The green – reduced crystal nano silver powder was characterized using XRD analysis, Zeta sizer, Scanning Electron Microscopy (SEM) equipped with Energy Dispersive Spectroscopy (EDS) in addition to Transmission Electron Microscopy (TEM). The synthesized crystal nano silver showed promising antibacterial activity against gram negative (*Escherichia coli*) and gram positive (*Staphylococcus aureus* and *Streptococcus*). The present study demonstrates the efficiency of synthesized nano silver as a cytotoxic agent against MCF-7 breast cancer cell line and HepG2 liver hepatocellular cancer cell line using by MTT assay. Thus, the synthesized crystal nano silver can be used as a wide range therapeutic agent against bacteria and cancer.

(Received September 27, 2015; October 28, 2015)

Keywords: Green Synthesis, Nano silver, Crystal Powder, Characterization, MTT, cytotoxicity and antibacterial

1. Introduction

Nanotechnology is a rapidly growing science of producing and utilizing nano-sized particles. A number of approaches are available for the synthesis of silver nanoparticles, such as thermal decomposition [1], electrochemical [2], microwave assisted process [3] and green chemistry [4]. Many of the nanoparticle synthesis or fabrication methods of nanoparticles involve the use of hazardous chemicals, low material conversions and high energy requirements. So, a growing need to develop an environmentally friendly process for nanoparticle (NPs) synthesis without using toxic chemicals and to makes nanoparticles more biocompatible and environmentally benign is gaining importance[5,6]. The green synthesis of Ag NPs involves three main steps, which must be evaluated based on green chemistry perspectives, including (1) selection of solvent medium, (2) selection of environmentally benign reducing agent, and (3) selection of nontoxic substances for the NPs stability [7]. Many plants such as *Pelargonium graveolens* [8], *Medicago sativa* [9], *Azadirachta indica* [10], *Lemongrass* [11], *Aloe vera* [12], *Cinnamomum Camphora* [13], *Emblca officinalis* [14], *Capsicum annum* [15], *Diospyros kaki* [16], *Carica papaya* [17], *Coriandrum sp.* [18], *Boswellia ovalifoliolata* [19], *Tridax procumbens*, *Jatropha curcas*, *Solanum melongena*, *Datura metel*, *Citrus aurantium* [20], and many weeds [21,22] have shown the potential of reducing silver nitrate to give formation of silver nanoparticles. AgNPs are among the promising nano

products that have gained increasing interest in the field of nanomedicine due to their structure and functional properties and obvious therapeutic potential in treating a variety of diseases [23]. AgNPs are also known for their antimicrobial potential against several other viruses, including hepatitis B [24], respiratory syncytial virus [25], and herpes simplex virus type 1 [26]. The use of silver as an antimicrobial agent is well recognized, however there are limited reports on its use as an antitumor agent; among these, there is a recent report on the anti-proliferative effect of silver nanoparticles on human glioblastoma cells (U251) [27]. Further, several studies shown cellular changes resulting from oxidative stress was produced by the generation of reactive oxygen species (ROS) in tumor cells, which increases the cytotoxicity activity of the drugs [28]. Although there is a wide range of cytotoxic agents used in the treatment of breast cancer, such as doxorubicin, cisplatin, and bleomycin, they have shown drawbacks in their use and are not as efficient as expected. Therefore, it is of great interest to find novel biocompatible therapeutic agents against cancer [29]. Thus, the present study was designed to develop a green, cost effective, rapid, and nontoxic method for synthesis of crystal AgNPs powder using CTAB and orange peel extract. In addition, green synthesized nano silver was evaluated potential cytotoxic effects in human breast cancer cells (MCF-7) using cell viability, and analysis of their antibacterial activity against gram negative (*Escherichia coli*) and gram positive (*Staphylococcus aureus* and *Streptococcus*) bacteria. To the best of our

knowledge, this is the first study describing the preparation of *crystal nano* silver powder using CTAB and orange peel extract and their biological effects.

2. Experimental

2.1. Chemicals Materials and bio extract

For crystal bio nano silver powder, the reagent in this work is analytical grade and is used as received without further purification. Silver nitrate (AgNO₃) from Techno Pharmchem, India is used. Cetyl trimethylammonium bromide from BDH Labortary supplies pool, BH151 TD, England. Orange peel was washed and cut into small pieces, then boiled with deionized water for 3min then filtered.

2.2. Synthesis of green crystal nano silver powder

We presented a new approach to produce green nano silver crystal powder. green nano silver were synthesized by adding 7 ml aqueous solution of orange peel extract to the aqueous solution of 2.0 x 10⁻³ mole/ L silver nitrate (AgNO₃) and 5.0 x 10⁻⁴ mole/ L (CTAB) cetyly trimethylammonium bromide (CTAB) under vigorous stirring at temperature 40 °C for 13 minutes at room temperature which have colorless. When adding the extract, the color changed from colorless to brown color. The change of color indicted the formation of the respective bio nano silver, then drying by air to produce green crystal nano silver powder.

2.3. Characterization of crystal bio nano silver

The synthesized crystal nano silver powder was characterized using UV-visible spectroscopy analyses with the help of Perkin Elmer UV-visible spectrometer Lambda 25, PerkinElmer, United Kingdom. The size of nanoparticles was analyzed through Zetasizer, Nano series, HT Laser, ZEN3600 from Molvern Instrument, UK, while Transmission electron microscopy (TEM) JEM-1011, JEOL, Japan has been employed to characterize the size, shape and morphologies of formed crystal nanosilver. Energy Dispersive Spectrometer (EDS) analysis was performed for the confirmation of elemental silver. Elemental analysis on single particles was carried out using Oxford Instrument, Incax-act, equipped with Scanning electron microscopy.

2.4. Antimicrobial screening

Antimicrobial activity of green crystal nanosilver powder was determined using disc diffusion assay method. Pure culture of gram negative (*Escherichia coli*) and gram positive (*staphylococcus aureus* and *Streptococcus*) of bacteria were used. Nutrient agar medium plates were prepared, sterilized and solidified. After solidification bacterial cultures were swabbed on these plates. The sterile discs were dipped in green crystal nano silver (5,

10, 15 µg/ml) and placed in the nutrient agar plate and kept for incubation at 37 °C for 24 hours, upon inhibitory activity a clearing zone around the wells was observed. The diameter of the clearing zones was measured in mm using the ruler scale. The experiments were repeated 3 times and mean values of zone diameter were presented [30].

2.5. Evaluation of cytotoxic effect

MCF-7 cells (human breast cancer cell line) were obtained from VACSERA Tissue Culture Unit. HepG2 cells (human cell line of a well differentiated hepatocellular carcinoma isolated from a liver biopsy of a male Caucasian aged 15 years) were obtained from the American Type Culture Collection (ATCC). Dimethyl sulfoxide (DMSO) and crystal violet were purchased from Sigma (St. Louis, Mo., USA). DMEM, HEPES buffer solution, L-glutamine and gentamycin were purchased from (Bio Whittaker © Lonza, Belgium). Crystal violet stain (1%) is composed of 0.5 % (w/v) crystal violet and 50 % methanol then made up to volume with distilled H₂O and filtered through a Whatmann No. 1 filter paper. The cytotoxicity assay was done in the Regional Center for Mycology and Biotechnology (RCMB), Al-Azhar University (Cairo, Egypt).

2.5.1. Cytotoxicity assay

The cells were propagated in Dulbecco's modified Eagle's medium (DMEM) supplemented with 10% heat-inactivated fetal bovine serum, 1% L-glutamine, HEPES buffer and 50 µg/ml gentamycin. All cells were maintained at 37°C in a humidified atmosphere with 5% CO₂ and were sub-cultured two times a week. Cell toxicity was monitored by determining the effect of the test samples on cell morphology and cell viability. For cytotoxicity assay, the cells were seeded in 96-well plate at a cell concentration of 1 x 10⁴ cells per well in 100 µl of growth medium. Fresh medium containing different concentrations of the test sample was added after 24 h of seeding. Serial two-fold dilutions of the tested chemical compound were added to confluent cell monolayers dispensed into 96-well, flat-bottomed microtiter plates (Falcon, NJ, USA) using a multichannel pipette. The microtiter plates were incubated at 37°C in a humidified incubator with 5% CO₂ for a period of 48 h. Three wells were used for each concentration of the test sample. The little percentage of DMSO present in the wells (maximal 0.1%) was found not to affect the experiment. After incubation of the cells for 24 h at 37°C, various concentrations of sample (100, 50, 25, 12.5, 6.25, 3.125 µl/100ul) were added, and the incubation was continued for 48 h and viable cells yield was determined by colourimetric method. In brief, after the end of the incubation period, media were aspirated and the crystal violet solution (1%) was added to each well for at least 30 minutes. The stain was removed and the plates were rinsed using tap water until all excess stain was removed. Glacial acetic acid (30%) was then added to all wells and mixed

thoroughly, and then the absorbance of the plates were measured after gently shaken on Microplate reader (TECAN, Inc.), using a test wavelength of 490 nm. All results were corrected for background absorbance detected in wells without added stain. Treated samples were compared with the cell control in the absence of the tested sample. All experiments were carried out in triplicate. The cell cytotoxic effect of each tested compound was calculated.

3. Results and discussion

3.1. Visual observations and UV-Visible spectral studies

Initial confirmation for synthesis of nano silver was confirmed by the formation of a brown color. Silver nanoparticles absorb radiation in the visible region of the electromagnetic spectrum (380–450 nm) due to the excitation of surface plasmon vibrations, and this is responsible for the brown color of nano silver in various media [31,32]

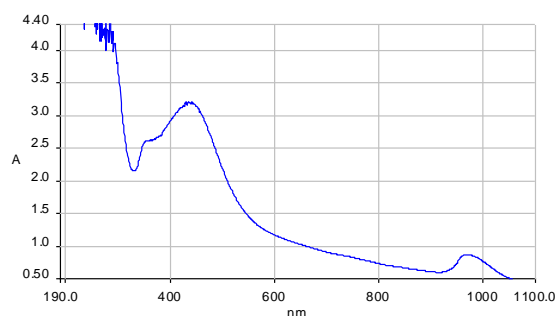


Fig. 1. UV-vis absorption spectrum of green crystal nano silver

The UV-vis spectra results are the most efficient method for detecting the formation of nanoparticles. The progress of the reaction leading to reduce of pure Ag^+ to nano silver was monitored by observing the color change and absorbance maxima peak in the range of 420–460 nm using UV-vis spectrophotometer [33]. The absorption peak was observed at 441.08 nm for the green crystal nano silver as shown in Fig. 1 which may be due to the formation of monodispersed and smaller sized NPs and the appearance of more than one peak is likely due to the formation of nanoparticles of various shapes and sizes [34]. The occurrence of absorption peak is due to the surface plasmon resonance (SPR) property of the metallic nanoparticles which occurs due to the oscillations of free electrons on the surface of the metallic nanoparticles when they align in resonance with the wavelength of irradiated light [35].

3.2. Particle size and distribution using DLS

Dynamic light scattering (DLS) was investigate the polydispersity index and average size of the synthesized

nanoparticles in a colloidal aqueous environment. When particles were dispersed in a medium, it exhibited Brownian motion measured by fluctuations in the intensity of scattered light in the system out of which translational diffusion co-efficient is calculated by applying the Stokes–Einstein equation that gives the hydrodynamic size of the particle [36]. The polydispersity index (PDI) is the measure of the width of the particle size distribution calculated from a cumulant analysis of the DLS measured intensity autocorrelation function where a single particle size is assumed and a single exponential fit is applied to the autocorrelation function [37]. The PDI value ‘0’ represents monodisperse distribution whereas value ‘1’ represents polydisperse distribution. Fig.2 showed the average size of the formed nano silver it was 2.866 nm with mono-dispersity which can be observed clearly from the one peak with an intensity 100% , diameter (3.146 nm) and width (1. 059 nm). This due to monodispersity of nanoparticles which gives very high stability of nanoparticles for a long time. In addition, the (PDI), which is 0.134, indicates high stability and homogeneity.

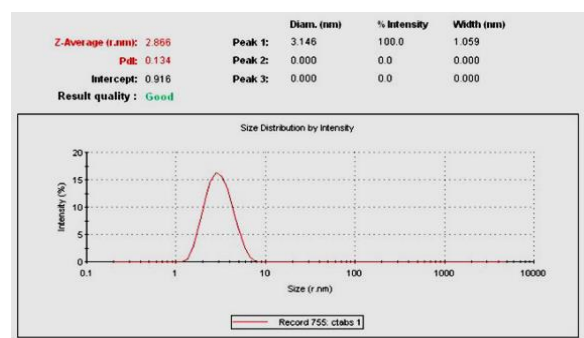


Fig. 2. Particle size distribution of green crystal nano silver

3.3. TEM analysis

TEM proved the formation of green crystal nano silver nanoparticles as shown in Fig. 3 which represented and indicates well dispersed particles. The TEM analysis revealed that the particle size of silver particles shows that the particle size ranges less than 50 nm. The nanoparticles predominantly adopt spherical and quasi-spherical morphologies with crystalline structure and a variety of sizes. These results were suitable with the zeta sizer and UV results.

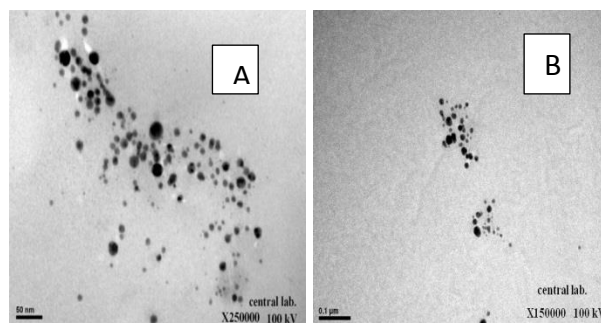


Fig. 3(A-B) show a graph of TEM images of green crystal nano silver

3.4. EDS and SEM analysis

EDS analysis gives qualitative as well as quantitative status of elements that may be involved in formation of nanoparticles. Fig. 4A shows elemental profile of synthesized nanoparticles using CTAB and orange peel extract and confirms the formation of silver nanoparticles and also shows counts at 3 keV due to silver nanoparticles. Generally metallic silver nanocrystals show typical optical absorption peak approximately at 3 keV due to surface plasmon resonance [38]. The elemental analysis of the silver nanoparticles shown a silver signal along with sodium peak, which may have originated from the biomolecules bound to the surface of the silver nanoparticles. It has been reported that nanoparticles synthesized using plant extracts are surrounded by a thin layer of some capping organic material from the plant leaf broth and are, thus, stable in solution long time after synthesis [39]. This is another advantage of nanoparticles synthesized using plant extracts over those synthesized using chemical methods. Fig. 4B illustrates the SEM image which showed a small white spots which represent of silver nanoparticles with spherical shaped.

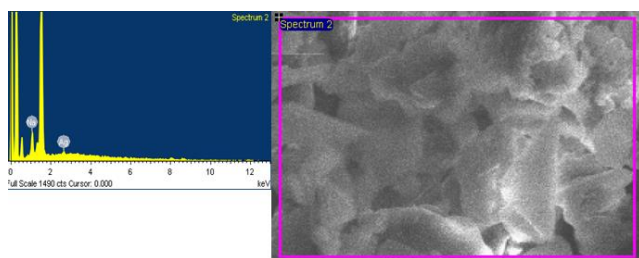


Fig. 4. EDS equipped with SEM presented the image and percentage of silver element in green nano suspension

3.5. Antibacterial property analysis

The antibacterial activity of green silver nanoparticles was found to utilize inhibitory effects on different species of bacteria: gram negative (*Escherichia coli*) and gram positive (*S. aureus* and *Streptococcus*). The inhibition zones obtained indicates maximum antibacterial activity of the prepared green crystal nanoparticles. The results show the green nano silver exhibited good antibacterial activity against both Gram-negative and Gram-positive bacteria (Fig. 5). But it showed higher antibacterial activity against *E. coli* than *S. aureus* and *Streptococcus* (Fig. 5A). This differential activity may possibly be due to the difference in bacterial cell wall structure. Cell wall of Gram-positive bacteria is composed of a thick layer of peptidoglycan that constitutes linear polysaccharides chains cross-linked by short peptides, thus forming rigid structure. This leads to difficulty in penetration of silver nanoparticles when compared to the Gram-negative bacteria where the cell wall possesses a much thinner layer of peptidoglycan [40].

In general, the mechanism of the inhibitory effects of Ag ions on microorganisms, is partially known. Some studies have reported that the positive charge on the Ag ion is crucial for its antimicrobial activity through the

electrostatic attraction between the negative charge on the cell membrane of microorganism and positively charged nanoparticles [41]. In contrast, Sondi and Salopek-Sondi [42] reported that the antimicrobial activity of silver nanoparticles on Gram-negative bacteria was dependent on the concentration of Ag nanoparticle, and was closely associated with the formation of the pits in the cell wall of bacteria. Ag nanoparticles accumulated in the bacterial membrane caused a change in the permeability, resulting in cell death. However, there studies included both positively charged Ag ions, and negatively charged Ag nanoparticles, it does not explain the antimicrobial mechanism of only the positively charged Ag nanoparticles. Therefore, we expect that there is another possible mechanism. (Amro et al, 2000) suggested that metal depletion may cause the formation of irregularly shaped pits in the outer membrane and change membrane permeability, which is caused by progressive release of lipopolysaccharide molecules and membrane proteins [43]. Also, Sondi and Salopek-Sondi speculate that a similar mechanism may cause the degradation of the membrane structure of *E. coli* during treatment with Ag nanoparticles [42]. Although the interference mechanism of AgNPs and bacteria involve some sort of binding mechanism, the level of that interaction between AgNPs and component(s) of the outer bacterial membrane is still not well understood.

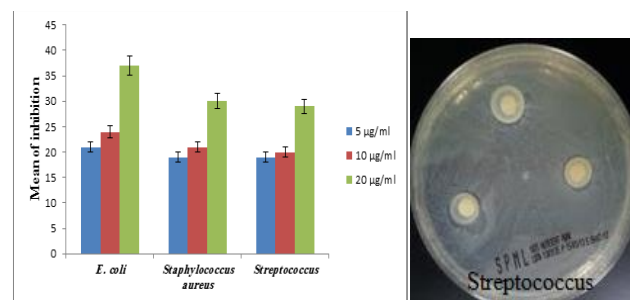
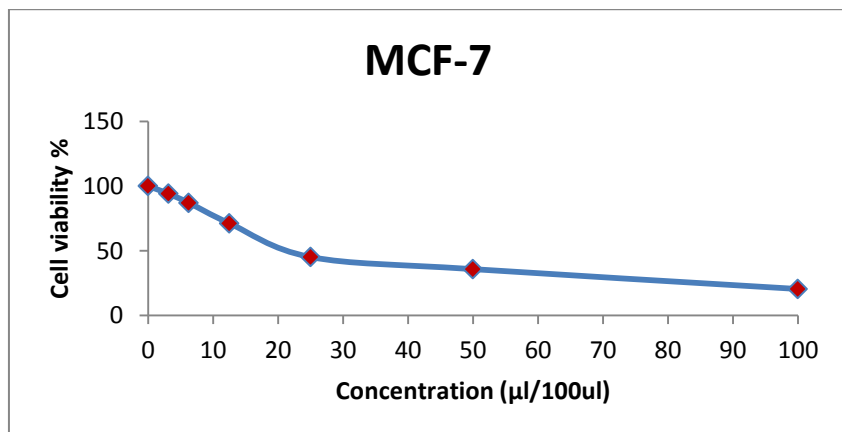


Fig. 5. Antibacterial activity assay of the green crystal nano silver against different bacteria strains

3.6. Standard cytotoxicity assays

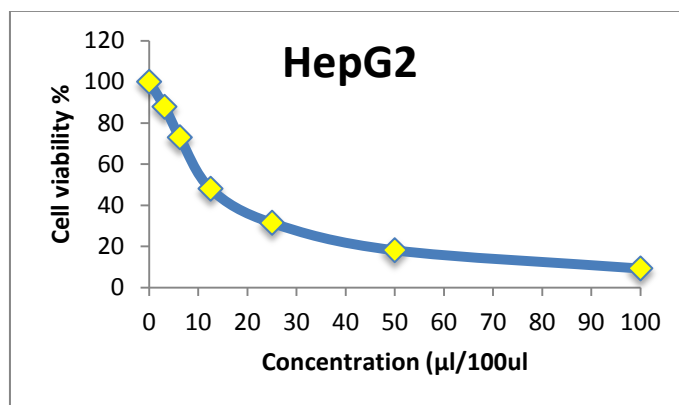
The cell viability assay is one of the important methods for toxicology analysis which explain the cellular response to a toxic materials and it can provide information on cell death, survival, and metabolic activities. In vitro cytotoxicity of the green crystal nano silver was estimated against human breast cancer MCF 7 cells and HepG2 liver hepatocellular carcinoma at different concentrations (100, 50, 25, 12.5, 6.25, 3.125 µl/100ul). Fig. 5 and 6 were show a dramatic increase in cell viability of MCF 7 and HepG2 when the concentration of nano silver was increased, with IC_{50} being $IC_{50} = 22.7$ and $IC_{50} = 11.99$ µl/100ul in case of MCF-7 and HepG-2 cell lines, respectively. In fact, silver nanoparticles may induce reactive oxygen species and cause damage to cellular components leading to cell death [39]. These results clearly presented the increased potential of green

synthesized crystal nano silver against cancer cells and this deserves further analysis.



Sample conc. (µl/100ul)	Viability % (3 Replicates)				Inhibition %	Standard Deviation (±)
	1 st	2 nd	3 rd	Mean		
100	23.14	20.07	18.34	20.52	79.48	2.43
50	37.45	34.91	35.23	35.86	64.14	1.38
25	48.29	42.85	44.52	45.22	54.78	2.79
12.5	70.12	71.92	71.83	71.29	28.71	1.01
6.25	87.64	86.56	86.97	87.06	12.94	0.55
3.125	93.76	94.64	93.88	94.09	5.91	0.48
0	100	100	100	100	0.00	

Fig. 6. Cytotoxic activity of green crystal nano silver suspension against MCF-7 cell line



Sample conc. (µl/100ul)	Viability % (3 Replicates)				Inhibition %	Standard Deviation (±)
	1 st	2 nd	3 rd	Mean		
100	10.85	8.76	8.12	9.24	90.76	1.43
50	18.94	16.04	19.31	18.10	81.90	1.79
25	30.94	31.5	31.79	31.41	68.59	0.43
12.5	43.29	52.76	47.85	47.97	52.03	4.74
6.25	72.25	70.99	75.74	72.99	27.01	2.46
3.125	89.72	84.75	88.97	87.81	12.19	2.68
0	100	100	100	100	0.00	

Fig. 8. Cytotoxic activity of green crystal nano silver suspension against HepG2 cell line

4. Conclusion

This study demonstrate an environmentally and low cost synthesis of small size nano silver using CTAB and orange peel extract. The formation of nano silver was determined by UV, zita sizer and completed the characterization by TEM, SEM and EDS techniques. Crystalline nano silver was successfully employed in both antibacterial and anticancer activity. Based on these findings, resulting nano silver may lead to valuable applications in various fields such as medicinal and as antibacterial agents.

Conflict of interest statement

We declare that we have no conflict of interest.

Acknowledgements

The authors extend their appreciation to the Deanship of Scientific Research at King Saud University for funding this work through research group no RGP- VPP-278.

References

- [1] S. Navaladian, B. Viswanathan, R. P. Viswanath, T. K. Varadarajan, *Nanoscale. Res. Lett.*, **2**, 44 (2007).
- [2] M. Starowicz, B. Stypula, J. Banas, *Electrochem. Commun.*, **8**(2), 227 (2006).
- [3] K. S. Sreeram, M. Nidin, B. U. Nair, *Bull. Mater. Sci.*, **31**(7), 937 (2008).
- [4] N. A. Begum, S. Mondal, S. Basu, R. A. Laskar, D. Mandal, *Colloids Surf. B*, **71**(1), 113 (2009).
- [5] P. Logeswari, S. Silambarasan, J. Abraham, *Scientia Iranica F* **20**(3), 1049 (2013).
- [6] K. Govindaraju, S. Tamilselvan, V. Kiruthiga, G. Singaravelu, *Journal of Biopesticides*, **3**(1), 394 (2010).
- [7] P. Raveendran, J. Fu, S. L. Wallen, *J Am. Chem. Soc.* **125**, 13940 (2003).
- [8] S. S. Shankar, A. Ahmad, M. Sastry, *Biotechnology Progress*, **19**(6), 1627 (2003).
- [9] J. L. Gardea-Torresdey, E. Gomez, J. R. Peralta-Videa, J. G. Parsons, H. Troiani, M. Jose-Yacaman, *Langmuir*, **19**(4), 1357 (2003).
- [10] S. S. Shankar, A. Rai, A. Ahmad, M. Sastry, *Journal of Colloid and Interface Science*, **275**(2), 496 (2004).
- [11] S. S. Shankar, A. Rai, A. Ahmad, M. Sastry, *Chemistry of Materials*, **17**(3), 566 (2005).
- [12] S. P. Chandran, M. Chaudhary, R. Pasricha, A. Ahmad, M. Sastry, *Biotechnology Progress*, **22**(2), 577 (2006).
- [13] J. Huang, Q. Li, D. Sun et al., *Nanotechnology*, **18**(10), Article ID 105104, 2007.
- [14] B. Ankamwar, C. Damle, A. Ahmad, M. Sastry, *Journal of Nanoscience and Nanotechnology*, **5**(10), 1665 (2005).
- [15] S. Li, Y. Shen, A. Xie et al., *Green Chemistry*, **9**(8), 852 (2007).
- [16] J. Y. Song, B. S. Kim, *Korean Journal of Chemical Engineering*, **25**(4), 808 (2008).
- [17] D. Jain, H. Kumar Daima, S. Kachhwaha, S. L. Kothari, *Digest Journal of Nanomaterials and Biostructures*, **4**(3), 557 (2009).
- [18] K. B. Narayanan, N. Sakthivel, *Materials Letters*, **62**(30), 4588 (2008).
- [19] S. Ankanna, T. N. V. K. V. Prasad, E. K. Elumalai, N. Savithamma, *Digest Journal of Nanomaterials and Biostructures*, **5**(2), 369 (2010).
- [20] P. Rajasekharreddy, P. U. Rani, B. Sreedhar, *Journal of Nanoparticle Research*, **12**(5), 1711 (2010).
- [21] N. Roy, A. Barik, *International Journal of Nanotechnology*, **4**, 95 (2010).
- [22] V. Parashar, R. Parashar, B. Sharma, A. C. Pandey, *Digest Journal of Nanomaterials and Biostructures*, **4**(1), 45 (2009).
- [23] R. Bhattacharya, P. Mukherjee, *Advanced Drug Delivery Reviews* **60**, 1289 (2008).
- [24] K. Kalishwaralal, S. BarathManiKanth, S. Ram Kumar Pandian, V. Deepak, S. Gurunathan, *Journal of Controlled Release* **145**, 76 (2010).
- [25] L. Lu, R. W. Sun, R. Chen, C. K. Hui, C. M. Ho, J. M. Luk, G. K. Lau, C. M. Che, *Antiviral Therapy* **13**, 253 (2008).
- [26] L. Sun, A. K. Singh, K. Vig, S. R. Pillai, S. R. Singh, *Journal of Biomedicine and Biotechnology* **4**, 149 (2008).
- [27] D. Baram-Pinto, S. Shukla, N. Perkas, A. Gedanken, R. Sarid, *Bioconjugate Chemistry* **40**, 1497 (2009).
- [28] P. V. Asha Rani, M. Prakash Hande, S. Valiyaveetil, *BMC Cell Biology* **10**, 65 (2009).
- [29] Sangiliyandi Gurunathan, Jae Woong Han, Ahmed Abdal Dayem, Vasuki Eppakayala, Jung Hyun Park, Ssang-Goo Cho, Kyung Jin Lee, Jin-Hoi Kim, *Journal of Industrial and Engineering Chemistry* **19**, 1600 (2013).
- [30] N. Savithamma, M. Linga Rao, K. Rukmini, P. Suvarnalatha, *International Journal of Chem Tech Research*, **3**, 1394 (2011).
- [31] M. Sastry, K. S. Mayya, V. Patil, D. V. Paranjape, S. G. Hegde, *Journal of Physical Chemistry B* **101**, 4954 (1997).
- [32] J. L. Gardea-Torresdey, E. Gomez, J. R. Peralta-Videa, J. G. Parsons, H. Troiani, M. Jose-Yacaman, *Langmuir* **19**, 1357 (2003).
- [33] Debasis Nayak, Sarbani Ashe, Pradipta Ranjan Rauta, Manisha Kumari, Bismita Nayak, *Materials Science and Engineering C* **58**, 44 (2016).
- [34] Kantrao Saware, Balaji Sawle, Basavraja Salimath, Kamala Jayanthi, Venkataraman Abbaraju, *International Journal of Research in Engineering and Technology* eISSN: 2319-1163 | pISSN: 2321-7308.
- [35] B. J. Wiley, S. H. Im, Z. Y. Li, J. McLellan, A. Siekkinen, Y. Xia, *J. Phys. Chem. B* **110**, 15666 (2006).
- [36] B. J. Frisken, *Appl. Opt.* **40**, 4087 (2001).
- [37] D. E. Koppel, *J. Chem. Phys.* **57**, 4814 (2003).

- [38] M. R. Bindhu, M. Umadevi, *Spectrochim. Acta Part A: Mol. Biomol. Spec.* **101**, 184 (2013).
- [39] J. Das, M. Paul Das, P. Velusamy, *Spectrochim. Acta Part A: Mol. Biomol. Spec.* **104**, 265 (2013).
- [40] S. Shrivastava, T. Bera, A. Roy, G. Singh, P. Ramachandrarao, D. Dash, *Nanotechnology* **18**, 225103 (2007).
- [41] T. Hamouda, A. Myc, B. Donovan, A. Shih, JD. Reuter, A. JR. Baker JR, *Microbiol Res*; **156**(1 -7), (2000).
- [42] I. Dragieva, S. Stoeva, P. Stoimenov, E. Pavlikianov, K. Klabunde, *Nanostruct Mater*; **12**, 267 (1999).
- [43] N. A. Amro, L. P. Kotra, K. Wadu-Mesthrige, Bulychev A, S. Mobashery, G. Liu, *Langmuir*; **16**, 2789 (2000).

*Corresponding authors: mawad@ksu.edu.sa, ahindi@ksu.edu.sa